arXiv:cond-mat/0407655v2 [cond-mat.mes-hall] 12 Nov 2004

Shot noise of inelastic tunneling through quantum dot systems

Bing Dong[1,2], H. L. Cui[1,3], X. L. Lei[2], and Norman J. M. Horing[1]
[1] *Department of Physics and Engineering Physics, Stevens Institute of Technology, Hoboken, New Jersey 07030*
[2] *Department of Physics, Shanghai Jiaotong University, 1954 Huashan Road, Shanghai 200030, China*
[3] *School of Optoelectronics Information Science and Technology, Yantai University, Yantai, Shandong, China*

We present a theoretical analysis of the effect of inelastic electron scattering on current and its fluctuations in a mesoscopic quantum dot (QD) connected to two leads, based on a recently developed nonperturbative technique involving the approximate mapping of the many-body electron-phonon coupling problem onto a multichannel single-electron scattering problem. In this, we apply the Büttiker scattering theory of shot noise for a two-terminal mesoscopic device to the multichannel case with differing weight factors and examine zero-frequency shot noise for two special cases: (i) a single-molecule QD and (ii) coupled semiconductor QDs. The nonequilibrium Green's function method facilitates calculation of single-electron transmission and reflection amplitudes for inelastic processes under nonequilibrium conditions in the mapping model. For the single-molecule QD we find that, in the presence of the electron-phonon interaction, both differential conductance and differential shot noise display additional peaks as bias-voltage increases due to phonon-assisted processes. In the case of coupled QDs, our nonperturbative calculations account for the electron-phonon interaction on an equal footing with couplings to the leads, as well as the coupling between the two dots. Our results exhibit oscillations in both the current and shot noise as functions of the energy difference between the two QDs, resulting from the spontaneous emission of phonons in the nonlinear transport process. In the "zero-phonon" resonant tunneling regime, the shot noise exhibits a double peak, while in the "one-phonon" region, only a single peak appears.

PACS numbers: 73.63.Kv, 71.38.-k, 73.50.Td

I. INTRODUCTION

Recent progress in nanotechnology has made possible the fabrication of single-electron tunneling devices using organic molecules, the size of which is sufficiently small so that the discrete nature of its energy levels is important. In contrast to semiconductor quantum dots (QD), the molecular materials possess much weaker elastic parameters, such that it is very easy to excite their internal vibrational degrees of freedom (phonon modes) when electrons are incident upon the molecule through a tunnel junction from an external environment. This can significantly influence electron tunneling at low temperature, and the phenomenon has now provoked a large amount of experimental[1,2,3,4,5] and theoretical[6,7,8,9,10,11] work on the problem of tunneling through a single level with strong coupling to local phonon modes.

On the other hand, phonon-asisted inelastic tunneling in semiconductor QDs has continued to attract extensive studies. In particular, a recent experiment has measured the nonlinear tunneling current through a tunable two-level quantum system, i.e., coupled semiconductor QDs (CQDs), at low temperature with the observation of robust spontaneous emission of phonons leading to an oscillatory structure in the current spectrum.[12] Following this, nonperturbative theoretical analyses ascribed this oscillation to an interference effect of the electron-phonon interaction (EPI) in CQDs.[13,14]

Thus far, most theoretical work concerning this inelastic tunneling problem has focused on calculating current through a two-terminal setup in dc and ac conditions. Only a few attempts have been made to study the current-current correlations (shot noise) in QD systems,[8,11,15] which has become a central subfield of mesoscopic physics.[16,17,18] In the present paper, we investigate low-frequency shot noise behavior when the QD is subject to strong coupling with a local phonon mode. This kind of strongly nonequilibrium problem has been found to be difficult to solve because previous studies demonstrated that when inelastic processes such as phonon emission and absorption are considered in the tunneling event through a QD, electron scattering becomes a strongly correlated many-body problem involving electrons and the various excited phonon states of the QD.[6,7,8,9,10,11,13,14] In this case, the usual perturbation theory is invalid for dealing with this scattering problem, albeit that it has been extensively exploited with enormous success to study conventional transport in bulk materials.

Recently, a nonperturbative scheme was proposed by Bonča and Trugman[19] to study the small polaron of the coupled electron-phonon system described by the Holstein model.[20] Later, this method was applied to the analysis of inelastic electron scattering in mesoscopic quantum transport in semiconductor QDs and molecular wires within the framework of the Landauer-Büttiker scattering theory.[21,22,23] Very recently, we advantageously employed this mapping scheme to evaluate time-dependent phonon-assisted tunneling at low temperature through a single-molecular QD with the help of the psuedo-operator technique and the nonequilibrium Green's function (NGF) method.[24] The fundamental idea is to remodel the strongly correlated Hamiltonian in terms of

the combined electron-phonon Fock space, mapping the many-body problem onto a one-body scattering problem (noninteracting system), which is highly desirable to facilitate an accurate calculation of the current-fluctuation spectrum.

However, this mapping technique introduces an additional difficulty: it also maps the ordinary single-mode leads in the two terminals onto pseudo-multi-channel leads associated with differing weight factors P_n corresponding to the statistical probability of the excited phonon number state n of the mesoscopic device. Consequently, the original Landauer current formula needs to be modified to properly account for this fact and the Pauli exclusion principle as it applies to multi-channel leads.[21,23,24] For example, if we consider a tunneling event in which an electron with energy ϵ enters from the nth channel of the left lead, scatters with a phonon in the QD, and finally exits into the mth channel of the right lead with energy ϵ', the contribution of this process to current is simply proportional to $P_n f_L^n(\epsilon)[1-f_R^m(\epsilon')]$ (f_η^l is the Fermi distribution function of the lth pseudochannel in lead η, as described in Section II below), multiplying the square modulus of the transmission amplitude, $|t_{Ln,Rm}|^2$. Correspondingly, it is clear that an analogous modification must be made in the Büttiker scattering formula for current-current correlations[16,17] in the presence of multichannel leads with differing weight factors. This issue is a central focus of this paper. In Section II, we will briefly present the appropriate generalization of scattering theory and provide the general formula for determining the zero-frequency shot noise spectrum of mesoscopic systems with EPI.

In two applications of this generalization we will examine low frequency electric current fluctuations as functions of voltage for the two cases mentioned above: 1) a single-molecular QD (single site) and 2) semiconductor CQDs (two sites) in the central region sandwiched between two normal leads. Every QD is taken to have only one single-particle energy level coupled with a dispersionless phonon mode of the Holstein-type model. Here we concentrate our attention on the effect of the inelastic scattering process in tunneling and ignore all other complexity of real molecular or semiconductor devices, except for EPI. For the single site case, our calculations predict (i) a step-type characteristic of the bias voltage-dependent shot noise analogous to the current-voltage curve at low temperature, in which the first step corresponds to resonance with the single level of the QD and the others result from phonon-emission-assisted resonances, and (ii) an enhancement of the Fano factor due to phonon effects in the high bias-voltage region.

For the two-site case, in order to observe the effect of spontaneous phonon emission, we consider an extraordinarily high bias-voltage between the two leads and calculate the current and shot noise as functions of the energy difference between the two QDs, which can be tuned experimentally using gate voltages. Very recently, the shot noise spectrum in CQDs was explored by means of master equations with correlation functions in Laplace transform space.[15] Under the physical presumption of weak tunneling between the QDs and leads, this method employed the noninteracting blip approximation to deal with the EPI.[13] Our objection here is to improve upon this by developing an approach which allows us to account for the EPI on an equal footing with the couplings to the leads, as well as treating the coupling between the two dots in a nonperturbative way. The mapping technique conforms to this purpose. Our calculations exhibit an oscillatory shoulder in the current and shot noise spectra due to spontaneous phonon emission in nonlinear transport. In the resonant tunneling regime, the shot noise has a double peak, while only a single peak shows up in the phonon-assisted resonant tunneling region.

The rest of this paper is arranged as follows. In Sec. II, we describe the class of systems that we study and present the appropriate generalization of scattering theory for calculating current fluctuations of a two-terminal device in the presence of EPI. In general, we find that the current fluctuation spectrum cannot be expressed in terms of transmission and reflection probabilities even in the zero frequency limit, but it is sensitive to the transmission and reflection amplitudes involving all pseudochannels. Our two applications occupy the following two sections: Sec. III for a single molecular QD and Sec. IV for the CQDs. In these two special cases, we employ the NGF technique to evaluate transmission and reflection amplitudes in the wide band limit. Numerical results and some discussions are also presented in these sections. Finally, our conclusions are summarized in Sec. V.

II. METHOD AND FORMULATION

A. Model and mapping Hamiltonian

Here, we consider the model of the two-terminal mesoscopic device as constituted of a central region (the device) connected to two noninteracting reservoirs via tunneling and coupled to a phonon bath. We assume that the two leads remain in local equilibrium with the Fermi distribution, $f_\eta(\omega)=[1+e^{(\omega-\mu_\eta)/k_BT}]^{-1}$ [μ_η is the chemical potential of the lead η ($=L$ or R), T is the temperature], and both of them have only one electronic channel. We also assume that the EPI takes place solely in the device and not in the ideal leads, specifically, there is no exchange between electrons and phonons in the tunneling processes. This is reasonable because high-order tunneling processes accompanied by phonon emission and absorption are much weaker than direct tunneling events. For simplicity, we adopt a single-mode Einstein-phonon with frequency ω_{ph}. Moreover, we neglect the spin degree of freedom and any effects of electron-electron Coulomb interactions.

Therefore, the Hamiltonian of this system involves three terms: $H = H_{\rm lead} + H_{\rm cen} + H_{\rm tl}$, where $H_{\rm lead}$ de-

scribes the two isolated leads, $H_{\rm cen}$ models the interacting central region in addition to the free-phonon contribution, and $H_{\rm tl}$ is the tunnel coupling between the leads and the device, respectively:

$$H_{\rm lead} = \sum_{\eta,k} \epsilon_{\eta k} c^\dagger_{\eta k} c_{\eta k}, \tag{1a}$$

$$H_{\rm cen} = H_d(\{d^\dagger_j\};\{d_j\}) + \hbar\omega_{ph} b^\dagger b - \sum_j \lambda_j d^\dagger_j d_j (b + b^\dagger), \tag{1b}$$

$$H_{\rm tl} = \sum_{\eta,k,j} V_{\eta,j}(c^\dagger_{\eta k} d_j + {\rm H.c.}). \tag{1c}$$

Here $c^\dagger_{\eta k}$ ($c_{\eta k}$) are the creation (annihilation) operators for the noninteracting electrons with momentum k and energy $\epsilon_{\eta k}$ in the lead η, and $\{d^\dagger_j\}$ ($\{d_j\}$) forms the complete and orthonormal set of single-electron creation (annihilation) operators in the central region, respectively. The form of H_d depends on geometry of the device being investigated. The last term in Eq. (1b) denotes the interaction of an electron on the central site with phonons: $b^\dagger$ (b) creates (destroys) a phonon, and λ_j is the on-site EPI constant. $V_{\eta,j}$ stands for the tunnel coupling between the device and the lead η.

Obviously, the model described by the above Hamiltonian (1) involves a many-body problem with phonon emission and absorption when the electron tunnels through the central region. Following the suggestion of Bonča and Trugman, we expand the electron states in the central region and the leads in terms of the direct product states composed of single-electron states and n-phonon Fock states:

$$|j,n\rangle = d^\dagger_j \frac{(b^\dagger)^n}{\sqrt{n!}}|0\rangle, \quad (n \geq 0) \tag{2}$$

and

$$|\eta k, n\rangle = c^\dagger_{\eta k} \frac{(b^\dagger)^n}{\sqrt{n!}}|0\rangle, \tag{3}$$

such that the electron state $|j\rangle$ in the central region and the state $|\eta k\rangle$ with momentum k in lead η, respectively, are accompanied by n phonons ($|0\rangle$ is the vacuum state). After performing this transformation, the many-body on-site EPI in Eq. (1b) can be mapped onto a one-body model:[19,21,22,23,24]

$$\sum_{j,n\geq 0} -\lambda_j \sqrt{n+1}(|j,n+1\rangle\langle j,n| + |j,n\rangle\langle j,n+1|)]. \tag{4}$$

In this procedure, the two noninteracting single-mode leads of Eq. (1a) are mapped to a multichannel model

$$\widetilde{H}_{\rm lead} = \sum_{\eta,k,n} \epsilon_{\eta k n} |\eta k, n\rangle\langle \eta k, n| \tag{5}$$

with $\epsilon_{\eta k n} = \epsilon_{\eta k} + n\hbar\omega_{ph}$. Here, the difference from traditional multi-channel leads lies in the fact that the channel index n represents the phonon quanta excited in the device, thus generating a weight factor $P_n = (1 - e^{-\beta\omega_{ph}})e^{-n\beta\omega_{ph}}$ [the statistical probability of the phonon number state $|n\rangle$ at finite temperature T ($\beta = 1/k_{\rm B}T$)], which must be associated with this channel. In this connection, we assume that the phonon bath is perpetually in thermal equilibrium, even under nonequilibrium transport conditions, due to a high energy relaxation rate. Thus, we ignore nonequilibrium phonon effects, considering phonon equilibration fast compared to the dwell time of an electron on the QD.[11] We also note that different channels are admixed with each other due to the EPI term, Eq. (4), which takes place solely in the central region. Finally, the tunneling part (1c) can also be rewritten in terms of this basis set:

$$\widetilde{H}_{\rm tl} = \sum_{\eta,k,j,n} V^n_{\eta,j}(|\eta k, n\rangle\langle j, n| + {\rm H.c.}). \tag{6}$$

$V^n_{\eta,j}$ is the coupling between the nth pseudochannel in lead η and the device. Clearly, the many-body EPI problem is transformed to a multichannel single-electron scattering problem with the help of the new representation, as illustrated in Fig. 1.

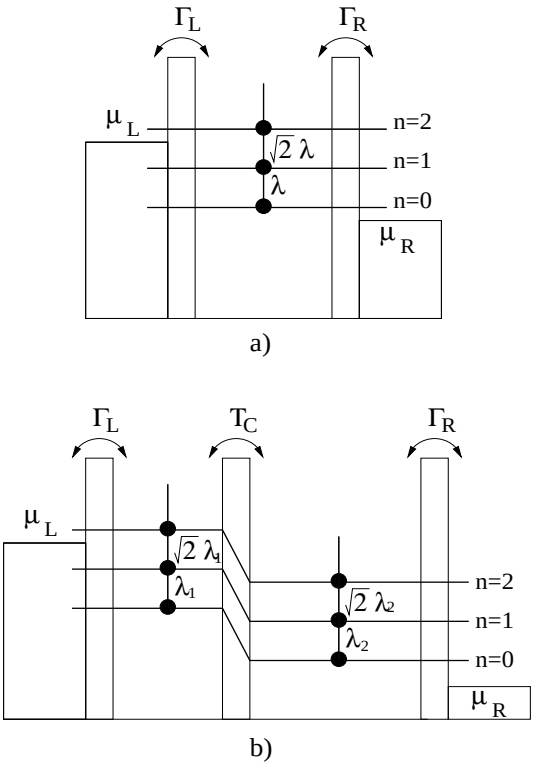


FIG. 1: Schematic description of the inelastic scattering problem for (a) a single site and (b) two sites in series, both with on-site EPI. Each phonon state of the site, taken jointly with the Bloch state of the electron in the lead, can be visualized as a pseudochannel labeled by n, which is connected to the two leads with hopping parameters $\Gamma_{L/R}$. These channels are connected vertically by the EPI, λ_j.

We depict the physical process of tunneling after re-

modeling the electron-phonon coupling system as follows: The nth pseudochannel in either the left or the right lead denotes an electron propagating in one of the single-electron modes of that lead with the device being in its n-phonon state. An electron incident on pseudochannel n in the left or right lead can transport elastically to the central region, where it then excites or absorbs m phonons and exits inelastically into the $(n \pm m)$th channel in the left or right lead; or experiences no exchange with phonon and exits elastically in the same channel in both leads. It is of central importance to note that, within this formulation, the many-body problem can be solved exactly and consequently there is no loss of phase coherence in the treatment of the electron-phonon exchange. Indeed, such coherent interference effects in the emission processes of phonons play a crucial role in nonlinear transport in CQDs. This is the reason that the present approach can provide a satisfactory description of the current spectrum consistent with actual experimental results.[12]

B. Current-current fluctuation spectra

In the section, we derive a general formula describing low-frequency current fluctuation spectra for a two-terminal mesoscopic device coupled to an Einstein-phonon bath (with frequency ω_{ph}). In the combined electron-phonon representation, the many-body problem becomes a one-body multichannel scattering problem, as described in the last section. With this picture in mind, we employ the Büttiker scattering approach to achieve this objective.[16,17]

First we introduce creation and annihilation operators of electrons for the incoming and outgoing states in all transverse channels. We employ creation, $a^\dagger_{\eta n}(\omega)$, and annihilation, $a_{\eta n}(\omega)$, operators for electrons with total energy ω incident upon the central region from channel n of lead η; and we employ the creation, $b^\dagger_{\eta n}(\omega)$, and annihilation, $b_{\eta n}(\omega)$, operators for electrons in the outgoing states. Clearly, they obey anticommutation relations.

In second quantized notation, we can write explicit forms for the wave function $\Psi_\eta(\mathbf{r},t)$ in lead η as:

$$\Psi_\eta(\mathbf{r},t) = \int d\omega e^{-i\omega t/\hbar} \sum_{n=1}^{N} \frac{\chi_{\eta n}(\mathbf{r}_\perp)}{(2\pi\hbar v_{\eta n}(\omega))^{1/2}} \times [a_{\eta n}(\omega) e^{ik_{\eta n} z} + b_{\eta n}(\omega) e^{-ik_{\eta n} z}]. \quad (7)$$

Here, $\chi_{\eta n}$ are the transverse parts of the electron wave functions [$\mathbf{r} = (\mathbf{r}_\perp, z)$], the wave vector in the nth channel of lead η is $k_{\eta n} = \hbar^{-1}[2m^*(\omega - n\hbar\omega_{ph})]^{1/2}$ (m^* is the effective electron mass), and the corresponding electron velocity is $v_{\eta n}(\omega) = \hbar k_{\eta n}/m^*$. N denotes the total phonon number, which is infinite in principle, but must truncated to a finite value for computational purposes. Correspondingly, we define the current operator as:

$$\hat{I}_\eta(z,t) = \frac{\hbar e}{2im} \int d\mathbf{r}_\perp \left[\Psi^\dagger_\eta(\mathbf{r},t) \frac{\partial}{\partial z} \Psi_\eta(\mathbf{r},t) - \left(\frac{\partial}{\partial z} \Psi^\dagger_\eta(\mathbf{r},t) \right) \Psi_\eta(\mathbf{r},t) \right]. \quad (8)$$

Substituting the wave function of Eq. (7) into this definition, and assuming that the velocities $v_{\eta n}(\omega)$ vary with energy quite slowly, the current operator can be simplified as:

$$\hat{I}_\eta(t) = \frac{e}{h} \sum_n \int d\omega d\omega' e^{i(\omega-\omega')t/\hbar} [a^\dagger_{\eta n}(\omega) a_{\eta n}(\omega') - b^\dagger_{\eta n}(\omega) b_{\eta n}(\omega')]. \quad (9)$$

In the scattering approach, the outgoing electron operators, b, are related to the incoming operators, a, via the $2N \times 2N$ scattering matrix $\boldsymbol{s}$:

$$\boldsymbol{s} = \begin{pmatrix} \boldsymbol{s}_{L,L} & \boldsymbol{s}_{L,R} \\ \boldsymbol{s}_{R,L} & \boldsymbol{s}_{R,R} \end{pmatrix} = \begin{pmatrix} \boldsymbol{r}_L & \boldsymbol{t}_L \\ \boldsymbol{t}_R & \boldsymbol{r}_R \end{pmatrix}, \quad (10)$$

in which all blocks have $N \times N$ dimensions. An element $s_{\eta n,\eta m}$ of the diagonal blocks describes a tunneling event in which an electron is incident from the ηm channel and reflects back to the nth channel in the same lead. For this reason we denote it as r_{Lnm} (r_{Rnm}), the reflection amplitude for the left (right) lead. Similarly, an element $s_{\eta n,\eta' m}$ ($\eta' \neq \eta$) of the off-diagonal blocks denotes electron transmission through the central region from the $\eta' m$ channel to the ηn channel; and these are the transmission amplitudes t_{Lnm} and t_{Rnm}. It should be noted that the scattering matrix is unitary $\boldsymbol{s}^\dagger \boldsymbol{s} = \boldsymbol{I}$ ($\boldsymbol{I}$ is the N-dimensional unit matrix) and symmetric. Therefore, we can express the current in terms of the operators a and $a^\dagger$ alone:

$$\hat{I}_\eta(t) = \frac{e}{h} \sum_{\alpha\beta,mn} \int d\omega d\omega' e^{\frac{i}{\hbar}(\omega-\omega')t} a^\dagger_{\alpha m}(\omega) \times A^{mn}_{\alpha\beta}(\eta;\omega,\omega') a_{\beta n}(\omega'), \quad (11)$$

where

$$A^{mn}_{\alpha\beta}(\eta;\omega,\omega') = \delta_{mn}\delta_{\alpha\eta}\delta_{\beta\eta} - \sum_l s^\dagger_{\eta m,\alpha l}(\omega) s_{\eta l,\beta n}(\omega'). \quad (12)$$

Proceeding to evaluation of the shot noise spectra, we recall that the noise power spectra between the leads η and η' can be expressed as the Fourier transform of the current-current correlation function:

$$S_{\eta\eta'}(\omega) = \frac{1}{2} \int_{-\infty}^{\infty} dt e^{i\omega(t-t')} [\langle \hat{I}_\eta(t) \hat{I}_{\eta'}(t') \rangle + \langle \hat{I}_{\eta'}(t') \hat{I}_\eta(t) \rangle - 2\langle \hat{I}_\eta(t) \rangle \langle \hat{I}_{\eta'}(t') \rangle], \quad (13)$$

where $\langle \cdots \rangle$ represents the quantum statistical average. Focusing attention on low-frequency noise in the same lead in the present paper, we obtain, after some algebra[16,17]

$$S_{\eta\eta}(0) = \frac{e^2}{h} \sum_{\alpha\beta,mn} \sum_{\mu\nu,kl} \int d\omega d\omega' A^{mn}_{\alpha\beta}(\eta;\omega,\omega)$$

$$\times A^{kl}_{\mu\nu}(\eta;\omega',\omega')\Big\{\langle a^\dagger_{\alpha m}(\omega)a_{\nu l}(\omega')\rangle\langle a_{\beta n}(\omega)a^\dagger_{\mu k}(\omega')\rangle$$
$$+\langle a^\dagger_{\mu k}(\omega')a_{\beta n}(\omega)\rangle\langle a_{\nu l}(\omega')a^\dagger_{\alpha m}(\omega)\rangle\Big\}. \quad (14)$$

Considering the fact that the channel actually corresponds to the phonon number state in this mapping model, these quantum statistical averages, $\langle a^\dagger a\rangle$, must be calculated with caution: an additional weight factor P_n must accompany any starting channel n jointly with the Fermi distribution, $f^n_\eta(\omega) = [1+e^{(\omega+n\hbar\omega_{ph}-\mu_\eta)/k_BT}]^{-1}$. Therefore, we have

$$S_{\eta\eta}(0) = \frac{e^2}{h}\sum_{\alpha\beta,mn}\int d\omega A^{mn}_{\alpha\beta}(\eta;\omega,\omega)A^{nm}_{\beta\alpha}(\eta;\omega,\omega)$$
$$\times\left\{P_m f^m_\alpha(\omega)[1-f^n_\beta(\omega)]+P_n f^n_\beta(\omega)[1-f^m_\alpha(\omega)]\right\}. \quad (15)$$

In contrast to the case without EPI, one can not further simplify the shot noise formula of Eq. (15) to write it in terms of transmission probabilities only without any detailed information concerning the device. Here, the shot noise formula for inelastic tunneling requires information about the transmission and reflection amplitudes of all pseudochannels. Actually, a similar result, that the noise can not be expressed in terms of the transmission probabilities only in the boson-field assisted tunneling, has been addressed in the studies of ac-driven current noise in quantum dots.[25] In the next two sections, we will apply this theory to evaluate zero-frequency shot noise in a single-molecular QD and semiconductor CQDs based on Eqs. (12) and (15).

It should be noted that since the mapping technique involves an underlying single-particle picture for the dot EPI, it does ignore the possibility of strong bath-dot many-body effects which could invalidate the single-particle picture, introducing broadening of tunneling associated with strong EPI and nonequilibrated phonon.[9,11] Such many-body effects are understood to play an important role in tunneling in the linear regime, but become trivial in the case of high bias-voltages, upon which this paper is focused.

III. A SINGLE-MOLECULAR QUANTUM DOT

A. Model and shot noise formula

In this section, we examine the EPI effects on the zero-frequency noise properties of a single-molecular QD. For this single-site case [shown in Fig. 1(a)], the Hamiltonian H_d of the central region becomes

$$H_d = \epsilon_d d^\dagger_1 d_1, \quad (16)$$

and summation with respect to the site index j reduces to only one term. In terms of the combined electron-phonon representation, we rewrite it as:

$$\widetilde{H}_d = \sum_{n\geq 0}(\epsilon_d + n\hbar\omega_{ph})|1,n\rangle\langle 1,n|. \quad (17)$$

As suggested by Haule and Bonča in their original work,[19] the transmission and reflection amplitudes in this single-site case can be obtained by solving the Schrödinger equation with trial wave functions. In our recent study of low-temperature time-dependent phonon-assisted tunneling through a single-molecular QD, we adopted the NGF method to compute the time-depdendent transmission probabilities within the framework of the mapping technique.[24] In fact, Fisher and Lee established a general relation between the scattering matrix elements and the retarded GFs of the conductor.[26] Hence, in the present paper we will employ the NGF technique to compute these transmission and reflection amplitudes in the wide band limit.

Following our previous paper,[24] we define pseudo-Fermi operators:

$$d^\dagger_{1n} = |1,n\rangle\langle 0|, c^\dagger_{\eta kn} = |\eta k,n\rangle\langle 0|. \quad (18)$$

and rewrite the mapping Hamiltonian in terms of these pseudoperators. The evaluation of the retarded GFs of the QD, $G^r_{mn}(t,t') \equiv i\theta(t-t')\langle\{d_{1m}(t),\ d^\dagger_{1n}(t')\}\rangle$, proceeds using the equation-of-motion technique. In the Fourier space, we have

$$[\omega-\epsilon_d-m\hbar\omega_{ph}-\Sigma^r_m(\omega)]G^r_{mn}(\omega)=\delta_{mn}$$
$$-\lambda_1\sqrt{m}G^r_{(m-1)n}(\omega)-\lambda_1\sqrt{m+1}G^r_{(m+1)n}(\omega), \quad (19)$$

where the retarded self-energy $\Sigma^r_m(\omega)$ due to coupling to the leads is defined as

$$\Sigma^r_m(\omega) = \sum_{\eta,k}\frac{|V_{\eta m}|^2}{\omega-\epsilon_{\eta k}-m\hbar\omega_{ph}+i0^+}. \quad (20)$$

In the wide band approximation, where the hopping matrix element $V^n_{\eta j} = V_{\eta j}$ is independent of energy, one has $\Sigma^r_m = -\frac{i}{2}(\Gamma_L+\Gamma_R)$ with $\Gamma_\eta = 2\pi\sum_k|V_\eta|^2\delta(\omega-\epsilon_{\eta k}-m\hbar\omega_{ph})$ as the generalized linewidth function. For simplicity, we assume the tunnel couplings between the molecular QD and the two leads to be symmetric $\Gamma_L = \Gamma_R = \Gamma$. Therefore, one can rewrite the resulting Eq. (19) in a compact matrix form:

$$[(\omega+i\Gamma)\boldsymbol{I}-\boldsymbol{B}]\boldsymbol{G}^r(\omega) = \boldsymbol{I}, \quad (21)$$

in which $\boldsymbol{B}$ is a $N\times N$ symmetrical tridiagonal matrix with $B_{nn} = \epsilon_d + n\hbar\omega_{ph}$, $B_{n(n-1)} = -\lambda\sqrt{n}$, and $B_{n(n+1)} = -\lambda\sqrt{n+1}$. A similar result is obtained for the advanced GF, $\boldsymbol{G}^a(\omega)$, and we have $\boldsymbol{G}^a = [\boldsymbol{G}^r]^\dagger$ in ω-space. The element G_{nn} corresponds to the probability amplitude of propagating in a state that starts and ends with the same number of n phonons, while an element G_{mn} $(n\neq m)$ denotes the probability amplitude of starting with m and ending with n phonons.

Furthermore, employing the Fisher-Lee relation:[26]

$$\boldsymbol{s}(\omega) = -\boldsymbol{I}+i\sqrt{\Gamma_L\Gamma_R}\boldsymbol{G}^r(\omega), \quad (22)$$

we immediately obtain the transmission and reflection amplitudes in the presence of a phonon bath:

$$s_{L(R)m,L(R)n} = r_{L(R)mn} = r_{mn} = -\delta_{mn}+i\Gamma G^r_{mn}(\omega),$$

$$s_{L(R)m,R(L)n} = t_{R(L)mn} = t_{mn} = i\Gamma G^r_{mn}(\omega). \quad (23)$$

It is easy to check that they obey properties (1) $\boldsymbol{r}^\dagger\boldsymbol{r} + \boldsymbol{t}^\dagger\boldsymbol{t} = \boldsymbol{I}$; (2) $\boldsymbol{r}^\dagger\boldsymbol{t} + \boldsymbol{t}^\dagger\boldsymbol{r} = 0$, due to the unitary property of the scattering matrix; and (3) $\boldsymbol{r} = -\boldsymbol{I} + \boldsymbol{t}$; (4) $2\boldsymbol{t}^\dagger\boldsymbol{t} = \boldsymbol{t}^\dagger + \boldsymbol{t}$.

Inserting the resulting transmission and reflection amplitudes, Eq. (23), into Eqs. (12) and (15), we obtain, after some algebra:

$$\begin{aligned} S_{LL}(0) = S_{RR}(0) = \frac{2e^2}{h}\int d\omega \sum_{mn} \{ &[(\boldsymbol{t}^\dagger\boldsymbol{t})_{mn}]^2 \\ &\times [P_n f^n_L(\omega)(1 - f^m_L(\omega)) + P_m f^m_R(\omega)(1 - f^n_R(\omega))] \\ &+ (\boldsymbol{r}^\dagger\boldsymbol{r})_{mn}(\boldsymbol{t}^\dagger\boldsymbol{t})_{mn}[P_n f^n_L(\omega)(1 - f^m_R(\omega)) \\ &+ P_m f^m_R(\omega)(1 - f^n_L(\omega))]\}, \end{aligned} \quad (24a)$$

and $S_{LR}(0) = S_{RL}(0) = -S_{LL}(0)$. We can also determine the elastic contribution to shot noise by imposing the constraint of elastic tunneling $m = n$:

$$\begin{aligned} S^{\rm el}_{LL}(0) = \frac{2e^2}{h}\int d\omega \sum_{n} \{ &(\boldsymbol{t}^\dagger\boldsymbol{t})_{nn} \\ &\times P_n[f^n_L(\omega)(1 - f^n_R(\omega)) + f^n_R(\omega)(1 - f^n_L(\omega))] \\ &- [(\boldsymbol{t}^\dagger\boldsymbol{t})_{nn}]^2 P_n[f^n_L(\omega) - f^n_R(\omega)]^2\}. \end{aligned} \quad (24b)$$

Thus, the total current I_L and its elastic part are given by:[21,24]

$$\begin{aligned} I_L = \frac{e}{h}\int d\omega \sum_{mn} &(\boldsymbol{t}^\dagger\boldsymbol{t})_{mn} \\ &\times \{P_n f^n_L(\omega)[1 - f^m_R(\omega)] - P_m f^m_R(\omega)[1 - f^n_L(\omega)]\}, \end{aligned} \quad (25a)$$

and

$$I^{\rm el}_L = \frac{e}{h}\int d\omega \sum_{n} (\boldsymbol{t}^\dagger\boldsymbol{t})_{mn} P_n[f^n_L(\omega) - f^n_R(\omega)]. \quad (25b)$$

Furthermore, the Fano factor, which measures the deviation from uncorrelated Poissonian noise, is defined as:

$$F = \frac{S_{LL}(0)}{2eI_L}. \quad (26)$$

B. Numerical results and discussions

In this subsection we address the numerical calculation of zero-frequency shot noise through a single-molecular QD in the presence of a phonon bath, on the basis of Eqs. (21), (23) and (24). For simplicity, we assume the bias voltage is distributed symmetrically, i.e., $+V/2$ on the left lead and $-V/2$ on the right lead. We also set the phonon energy $\omega_{ph} = 1$ as the unit of energy throughout the rest of the paper and choose the Fermi levels of the two leads as the reference of energy $\mu_L = \mu_R = 0$ at equilibrium. Other parameters in our calculations for the single-molecular QD are: $\lambda = 0.5$, $\Gamma = 0.04$, and $T = 0.04$.

It should be emphasized that the present approach is an *exact* method to deal with an interacting electron-phonon system having arbitrary coupling strength if the maximum number of phonons N_{ph} involved in the calculation is taken up to infinity. Unfortunately this is impossible in a real calculation and we have to truncate this number to a finite value chosen to insure computational convergence with desired accuracy. The appropriate value of N_{ph} depends on the energy of the Einstein-phonon mode, the EPI constant, and the temperature of the system under investigation. For the parameters involved in the present paper, we choose $N_{ph} = 8$ to obtain results with accuracy better than 1% in this and next sections.

In Fig. 2 we plot the total and elastic currents (a) and shot noises (b) as functions of the bias voltage V. For comparison, we also plot the current and shot noise for the same system without the EPI as dashed lines. Obviously, the shot noise and current have similar step characteristics with increasing bias-voltage. When the electron is not coupled to the phonon mode, only one step structure occurs when the bias-voltage matches the Fermi energy of the left lead with the single level in the QD, leading to the single peak in the differential conductance dI/dV and the differential shot noise dS/dV shown in Fig. 2(c). In the presence of a phonon bath, we find that: (1) The overall spectra are both shifted by λ^2/ω_{ph} due to the polaron effect (for instance, the main peaks in dI/dV vs. V and dS/dV vs. V corresponding to resonance with the QD level shift from the position $V/2 = \epsilon_d$ to $\epsilon_d - \lambda^2/\omega_{ph}$, with slightly suppressed amplitudes); and (2) new resonant peaks separated by the frequency of the phonon mode, $\hbar\omega_{ph}$, appear due to emission of phonons, indicating that a new pseudochannel has opened and participates in contributing to tunneling.

Figure 3 shows the bias-dependent Fano factor for the system under study. Roughly speaking, it is known that the current fluctuation for a noninteracting two-terminal conductor is $\sum_n T_n(1 - T_n)$ at zero temperature, and the corresponding Fano factor F is proportional to $\sum_n T_n(1 - T_n)/\sum_n T_n$, where T_n is the transmission probability of channel n.[16,17] Therefore, there is no current noise if the transmission probability is $T_n = 0$ or 1, and the Fano factor is correspondingly equal to $F = 1$ or 0, respectively. This is case in the low bias-voltage region, below the single-level resonance. In contrast, in the high bias-voltage limit, the Fano factor tends to $\frac{1}{2}$ for a symmetric noninteracting system, $\Gamma_L = \Gamma_R$. In addition, we observe that the Fano factor is significantly enhanced and exhibits more fine structure due to phonon effects in this region, in comparison with the uncorrelated noise.

IV. DOUBLE QUANTUM DOTS

Finally, we examine nonlinear transport and fluctuations in semiconductor CQDs in a series arrangement, for which $V^n_{L2} = V^n_{R1} = 0$. As shown in Fig. 1(b), the

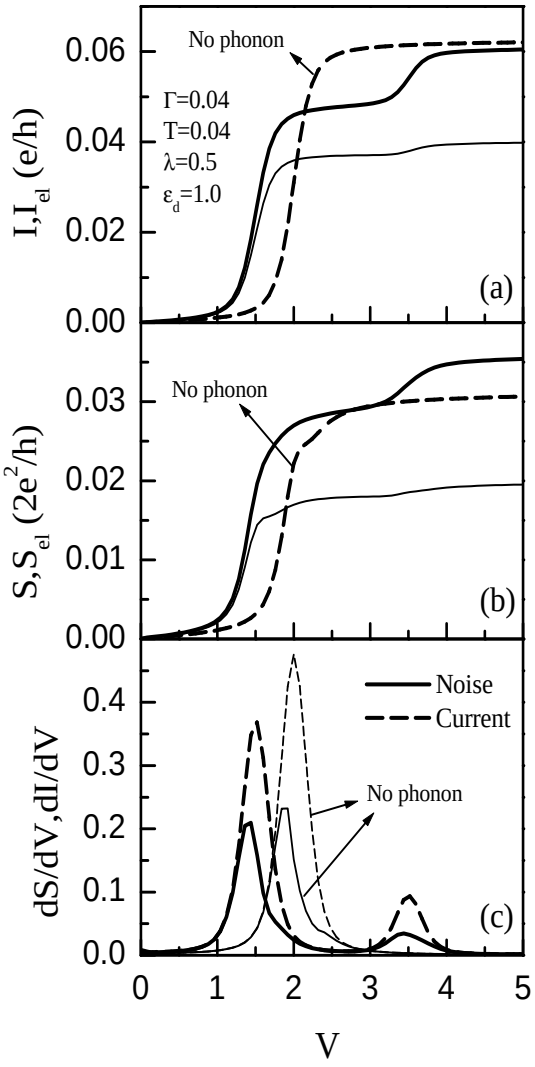


FIG. 2: (a) The calculated total current I (thick line), elastic current $I^{\rm el}$ (thin line); (b) the zero-frequency shot noise S (thick line), its elastic part $S^{\rm el}$ (thin line); and (c) the corresponding differential conductance dI/dV (dashed line) and differential shot noise dS/dV (solid line) as functions of applied bias voltage for a single-molecular QD with bare level $\epsilon_d = 1.0$. For comparison, we also plot the current and shot noise in the case without the phonon bath. The other parameters used in calculation are: $\Gamma = 0.04$, $\omega_{ph} = 1.0$, and $\lambda = 0.5$. The temperature is set to $T = 0.04$.

Hamiltonian H_d for the two-site case is given by:

$$H_d = \sum_{j=1,2} \epsilon_j d_j^\dagger d_j - T_c(d_1^\dagger d_2 + \text{H.c.}), \tag{27}$$

where T_c denotes the tunnel coupling between the two QDs. In terms of the joint electron-phonon representation, it becomes:

$$\begin{aligned}\widetilde{H}_d &= \sum_{j,n\geq 0} (\epsilon_j + n\hbar\omega_{ph})|j,n\rangle\langle j,n| \\ &\quad - \sum_{n\geq 0} T_c(|1,n\rangle\langle 2,n| + \text{H.c.}).\end{aligned} \tag{28}$$

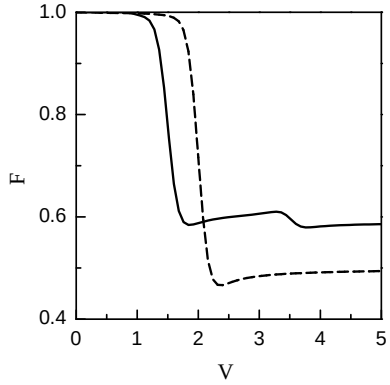


FIG. 3: Fano factor vs. bias-voltage V. Solid line denotes results with EPI, while the dashed line denotes results without EPI. The parameters are the same as in Fig. 2.

We also ignore higher-order tunneling processes by assuming that coherent electron transfer between the two QDs, governed by T_c, does not explicitly involve electron-phonon exchange. Correspondingly, the retarded GFs can be written in a block-matrix form:

$$\begin{aligned}&\begin{pmatrix} \boldsymbol{G}^r_{11}(\omega) & \boldsymbol{G}^r_{12}(\omega) \\ \boldsymbol{G}^r_{21}(\omega) & \boldsymbol{G}^r_{22}(\omega) \end{pmatrix} = \\ &\begin{pmatrix} (\omega + i\Gamma_L)\boldsymbol{I} - \boldsymbol{B}_1 & \boldsymbol{C} \\ \boldsymbol{C} & (\omega + i\Gamma_R)\boldsymbol{I} - \boldsymbol{B}_2 \end{pmatrix}^{-1},\end{aligned} \tag{29}$$

in which $\boldsymbol{B}_j$ $(j = 1, 2)$ is a $N \times N$ symmetrical tridiagonal matrix: $B_{j,nn} = \epsilon_j + n\hbar\omega_{ph}$, $B_{j,n(n-1)} = -\lambda_j\sqrt{n}$, and $B_{j,n(n+1)} = -\lambda_j\sqrt{n+1}$, and $\boldsymbol{C}$ is a N-dimensional diagonal matrix $C_{mn} = -\delta_{mn}T_c$. Once again, we can write the transmission and reflection amplitudes through the CQDs in terms of the retarded GFs, $\boldsymbol{G}^r_{ij}(\omega)$:

$$\begin{aligned}s_{L(R)m,L(R)n} &= r_{L(R)mn} = -\delta_{mn} + i\Gamma G^r_{11(22),mn}(\omega), \\ s_{L(R)m,R(L)n} &= t_{R(L)mn} = i\Gamma G^r_{12(21),mn}(\omega).\end{aligned} \tag{30}$$

Considering the properties of the matrices involved, we simplify the total current I_L as:

$$\begin{aligned}I_L &= \frac{e}{h}\int d\omega \sum_{mn} \Big\{(\boldsymbol{t}_L^\dagger \boldsymbol{t}_L)_{mn} P_n f_L^n(\omega)(1 - f_R^m(\omega)) \\ &\quad -(\boldsymbol{t}_R^\dagger \boldsymbol{t}_R)_{nm} P_m f_R^m(\omega)(1 - f_L^n(\omega))\Big\} \\ &= \frac{e}{h}\int d\omega \sum_{mn} (\boldsymbol{t}_L^\dagger \boldsymbol{t}_L)_{mn} \{P_n f_L^n(\omega)(1 - f_R^m(\omega)) \\ &\quad -P_m f_R^m(\omega)(1 - f_L^n(\omega))\}.\end{aligned} \tag{31}$$

Furthermore, the zero-frequency shot noise $S_{LL}(0)$ is given by

$$\begin{aligned}S_{LL}(0) &= \frac{2e^2}{h}\int d\omega \sum_{mn} \Big\{|(\boldsymbol{t}_L^\dagger \boldsymbol{t}_L)_{mn}|^2 \, [P_n f_L^n(\omega) \\ &\times(1 - f_L^m(\omega)) + P_m f_R^m(\omega)(1 - f_R^n(\omega))] \\ &+|(\boldsymbol{t}_R^\dagger \boldsymbol{r}_L)_{mn}|^2 [P_n f_L^n(\omega)(1 - f_R^m(\omega)) \\ &+P_m f_R^m(\omega)(1 - f_L^n(\omega))]\},\end{aligned} \tag{32}$$

and also $S_{LR}(0) = S_{RL}(0) = -S_{LL}(0) = -S_{RR}(0)$. Their elastic contributions can be obtained by setting $m = n$.

To compare this theoretical analysis with experimental results, we numerically calculate the current and shot noise based on Eqs. (31) and (32) as functions of the energy difference between the two QDs, $\varepsilon = \epsilon_1 - \epsilon_2$, which can be tuned by varying the gate voltage. We address only the case of high bias-voltage, $V = \mu_L - \mu_R \gg 0$. While the present formalism is valid for arbitrary choice of coupling parameters, tunneling strengths Γ and T_c, as well as EPI constants $\lambda_{1(2)}$, we specialize in the interest of comparison with the CQD experiments,[12] choosing these parameters as: $\Gamma_L = \Gamma_R = \Gamma = 0.25$, $T_c = 0.25$, $\lambda_1 = -\lambda_2 = \lambda = 0.1875$, and temperature $T = 0.125$ ($\omega_{ph} = 1$). In our calculations we set $eV = 10$ so that $\mu_L \gg \epsilon_1, \epsilon_2 \gg \mu_R$, in which case nonlinear transport does not significantly depend on μ_L and μ_R at low temperatures.

In Fig. 4(a), we plot the resulting currents, including the total current, its elastic and inelastic components, and the current without EPI, as functions of energy difference, ε. The external voltage, V, gives rise to a finite tunneling current through the CQDs. In the case without EPI, one can observe a single maximum in the current spectrum at $\varepsilon = 0$, i.e., the resonance point at which the energy level of the left dot is matched with that of the right dot, and there is a rapid decrease upon departure from this point. In contrast, the inelastic current due to phonon coupling is remarkably enhanced on the positive branch of the energy difference, $\varepsilon > 0$, in which phonons are emitted during the tunneling process. One can even unambiguously observe some peaks when the condition for spontaneous phonon-emission-assisted resonance, $\varepsilon = n\hbar\omega_{ph}$ ($n = 1, 2$ in our figure), is satisfied. However, for negative energy gap, $\varepsilon < 0$, the contribution of phonon absorption processes to inelastic current is negligible because there are not enough phonons available to be absorbed at low temperature. Moreover, our calculations predict a shoulderlike structure for $\varepsilon < 0$, which arises solely from elastic channels in the presence of the phonon bath.

It should be mentioned that the asymmetric and oscillatory shoulder behaviors in the current spectrum have also been obtained by means of the master equation[13] and the nonperturbative real-time renormalization-group (RTRG) method.[14] Nevertheless, the assumption taken in the master equation method (i.e., weak tunnel coupling) limits its validity for analysis of the current spectrum at stronger values of interdot coupling, T_c. Albeit the RTRG approach has not such limitation, this problem was not actually studied in Ref. [14]. Once again, we emphasize that our studies also assume the phonon bath to be in thermal equilibrium perpetually. Treatment of nonequilibrium phonon effects for CQDs is beyond the scope of the present paper. However, one of the advantages of the present scheme is that it treats the internal tunneling, T_c, on an equal footing with the couplings to the leads as well as EPI. Thus, it allows us to calculate the current spectrum for arbitrary internal tunneling strength, T_c. Such evaluations are exhibited in Fig. 4(b). With increasing T_c, the inelastic-resonance-induced oscillating shoulder structure is gradually smeared out, in agreement with experimental observations.[12]

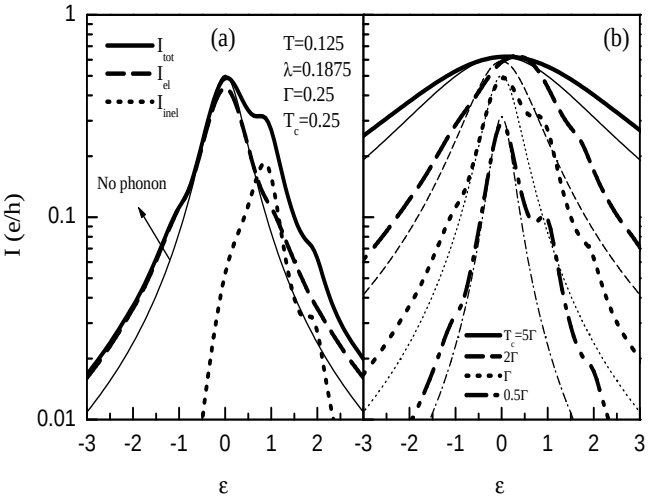


FIG. 4: Predicted tunneling current as a function of the energy difference, ε. (a) The total current $I_{\rm tot}$, its elastic component $I_{\rm el}$, its inelastic part $I_{\rm inel}$, and the current without phonon bath (thin line) vs. ε (with $\Gamma = T_c = 0.25$, EPI constants $\lambda_1 = -\lambda_2 = 0.1875$, and temperature $T = 0.125$); (b) The total currents (thick lines) and currents without EPI (thin lines) for various couplings, T_c, between the two QDs.

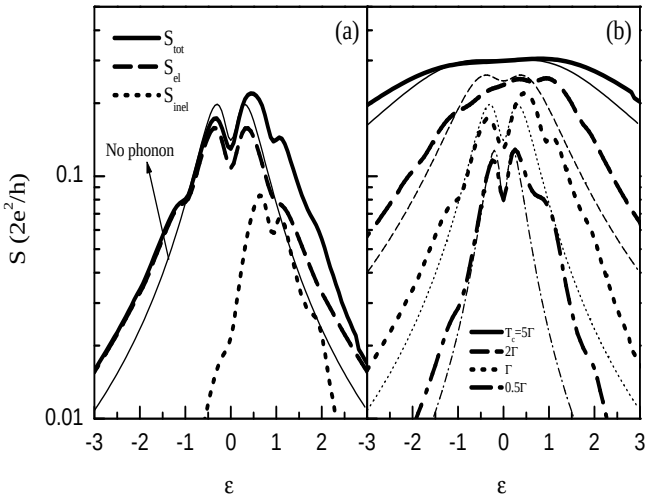


FIG. 5: Zero-frequency shot noise vs. ε. (a) Total shot noise, $S_{\rm tot}$; its elastic part, $S_{\rm el}$; its inelastic part, $S_{\rm inel}$; and shot noise with no EPI (thin line). The parameters are the same as in Fig. 4(a); (b) Shot noise with (thick lines) and without (thin lines) EPI for several different values of T_c.

In regard to zero-frequency shot noise, our evaluations are summarized in Fig. 5. In Fig. 5(a), where we plot the calculated shot noise spectra for the same system studied in Fig. 4(a), we see that the shot noise without EPI (thin

curve) exhibits two peaks located symmetrically around the resonant point, $\varepsilon = 0$. This behavior is due to the fact that there is no noise generation when the transmission probability is $T_{tr} = 0$ or 1, while maximal generation occurs between these values. In contrast to this, we find that phonon coupling enhances the shot noise peak located at the positive ε-side ($\varepsilon > 0$), but reduces the peak on the negative side, leading to breakdown of the symmetric structure. Moreover, interference of the EPI in the CQDs gives rise to oscillatory shoulders. It should be noted that, since the transmission probability corresponding to these inelastic resonances is small, the shot noise spectrum exhibits only a single peak rather than two peaks in the phonon-assisted resonant tunneling region.

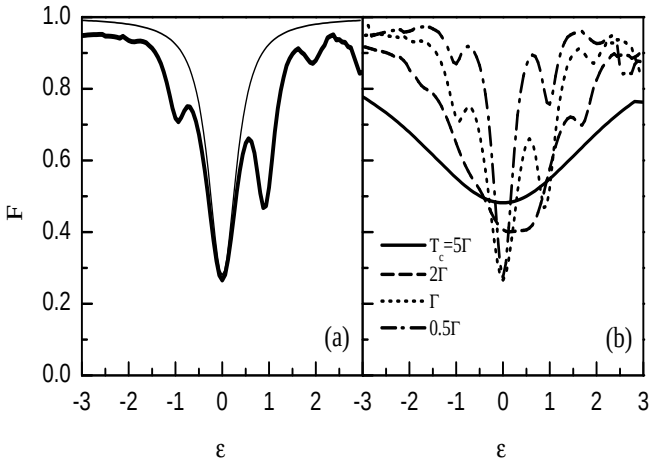


FIG. 6: Fano factor vs. ε. (a) Fano factors with (thick curve) and without (thin curve) EPI for the same system as in Fig. 4(a); (b) Fano factors for several different values of T_c.

The resulting Fano factor is plotted as a function of the energy gap, ε, in Fig. 6. At the elastic resonance point, $\varepsilon = 0$, the smallest Fano factor is observed, implying that quantum coherence significantly suppresses shot noise. For inelastic resonant tunneling, spontaneous phonon emission processes also reduce shot noise, which induces additional dips in the Fano factor for $\varepsilon > 0$. Interestingly, our results predict fine structure in the negative branch of ε. This is due to the shoulders in the current and shot noise spectra stemming from the contributions of elastic channels. It indicates that the Fano factor is quite sensitive to the interaction with phonons. Moreover, for large $|\varepsilon|$, the shot noise is dominated by the Poisson process, i.e., Fano factor $F \to 1$. Finally, increasing the interdot tunneling, T_c, progressively smooths out the shot noise spectra and the Fano factors as displayed in Figs. 5(b) and 6(b).

V. CONCLUSIONS

In summary, we have formulated a method that is well suited for the analysis and numerical evaluation of inelastic tunneling and the determination of the nonequilibrium zero-frequency shot noise spectra of mesoscopic devices in the presence of a dispersionless phonon bath at low temperature. Following the original work of Bonča and Trugman, we transformed the many-body EPI problem onto a one-body scattering problem, by projecting the original Hamiltonian in the representation of the joint coupled electron-phonon Fock space, i.e., the direct-product states of electron states and phonon number states. Based on this noninteracting Hamiltonian, we applied the Büttiker scattering theory of noise correlations in a two-terminal mesoscopic conductor to the case of pseudo-multi-channel leads with differing weight factors. Furthermore, we derived the formula for zero-frequency current-current fluctuations in terms of transmission and reflection amplitudes by properly taking account of the appropriate weight factors for the various starting channels.

It is appropriate to remark that the present approach to EPI is based entirely on an approximate mapping to a one-electron picture providing that the bath is not strongly perturbed (if that should occur, then bath-dot many-body effects would enter the problem and invalidate the one-electron picture). It is believed that this approximation is valid only in the high bias-voltage region. Indeed, the main purpose of this paper is to analyze zero-frequency shot noise for inelastic tunneling under nonlinear transport conditions. An important advantage of this technique is that it does not involve any restrictions on the parameters, so that it provides a reliable solution for arbitrary EPI constants and tunneling strengths to the leads, as well as arbitrary internal tunnel couplings.

Moreover, we have employed the derived formulae to analyze the shot noise properties of a single-molecular QD and for semiconductor CQDs in a series arrangement at low temperature. For this purpose, the NGF method provided a convenient tool to calculate the transmission and reflection amplitudes in the wide band approximation with the help of the Fisher-Lee relation. Some of the important findings of our work follow: For the single-molecule QD, the differential shot noise displays a peak-structure similar to that of the differential conductance as a function of increasing bias-voltage due to elastic and inelastic resonances. The Fano factor is enhanced due to EPI effects in the moderately high bias-voltage region. In the case of coupled QDs, both the current and shot noise spectra exhibit oscillatory shoulders as functions of the energy difference between the two QDs in the positive branch, stemming from spontaneous emission of phonons in nonlinear transport. In the elastic resonant tunneling region, the shot noise exhibits a double peak, however only a single peak shows up in the inelastic resonant tunneling region. The Fano factor is quite sensitive to the EPI.

Acknowledgments

B. Dong, H. L. Cui, and N. J. M. Horing are supported by the DURINT Program administered by the US Army Research Office. X. L. Lei is supported by Major Projects of National Natural Science Foundation of China, the Special Funds for Major State Basic Research Project (G20000683) and the Shanghai Municipal Commission of Science and Technology (03DJ14003). B. Dong thanks K. Flensberg for useful email correspondence and discussions.

[1] J. Chen, M. Reed, A. Rawlett, and J. Tour, Science **286**, 1550 (1999).
[2] W. Liang, M.P. Shores, M. Brockrath, J.R. Long, and H. Park, Nature **417**, 725 (2002)
[3] J. Park, A.N. Pasupathy, J.I. Goldsmith, C. Chang, Y. Yaish, J.R. Petta, M. Rinkoski, J.P. Sethna, H. Abruna, P.L. McEuen, and D.C. Ralph, Nature **417**, 722 (2002).
[4] H. Park, J. Park, A. Lim, E. Anderson, A. Allvisatos, and P. McEuen, Nature **407**, 57 (2000); Lam H. Yu and D. Natelson, Nano Lett. **4**, 79 (2004).
[5] N.B. Zhitenev, H. Meng, and Z. Bao, Phys. Rev. Lett. **88**, 226801 (2002).
[6] D. Bose and H. Schoeller, Europhys. Lett. **54**, 668 (2001); A.S. Alexandrov and A.M. Bratkovsky, Phys. Rev. B **67**, 235312 (2003); K.D. McCarthy, N. Prokof'ev, and M.T. Tuominen, Phys. Rev. B **67**, 245415 (2003).
[7] U. Lundin and R.H. McKenzie, Phys. Rev. B **66**, 75303 (2002).
[8] J.X. Zhu and A.V. Balatsky, Phys. Rev. B **67**, 165326 (2003).
[9] K. Flensberg, Phys. Rev. B **68**, 205323 (2003).
[10] S. Braig and K. Flensberg, Phys. Rev. B **68**, 205324 (2003).
[11] A. Mitra, I. Aleiner, and A.J. Millis, Phys. Rev. B **69**, 245302 (2004).
[12] T. Fujisawa, T.H. Oosterkamp, W.G. van der Wiel, B.W. Broer, R. Aguado, S. Tarucha, Leo P. Kouwenhoven, Science **282**, 932 (1998).
[13] T. Brandes and B. Kramer, Phys. Rev. Lett. **83**, 3021 (1999); T. Brandes, N. Lambert, Phys. Rev. B **67**, 125323 (2003)
[14] M. Keil and H. Schoeller, Phys. Rev. B **66**, 155314 (2002).
[15] R. Aguado and T. Brandes, Phys. Rev. Lett. **92**, 206601 (2004).
[16] M. Büttiker, Phys. Rev. B **46**, 12485 (1992).
[17] For an overview of the shot noise problem, please refer to Ya.M. Blanter and M. Büttiker, Phys. Rep. **336**, 1 (2000).
[18] B. Dong and X.L. Lei, J. Phys.: Cond. Matter **14**, 4963 (2002).
[19] J. Bonča and S.A. Trugman, Phys. Rev. Lett. **75**, 2566 (1995).
[20] T. Holstein, Ann. Phys. (N.Y.) **8**, 325 (1959).
[21] K. Haule and J. Bonča, Phys. Rev. B **59**, 13087 (1999).
[22] H. Ness and A.J. Fisher, Phys. Rev. Lett. **83**, 452 (1999)
[23] E.G. Emberly and G. Kirczenow, Phys. Rev. B **61**, 5740 (2000).
[24] B. Dong, H.L. Cui, and X.L. Lei, Phys. Rev. B **69**, 205315 (2004).
[25] S. Camalet, J. Lehmann, S. Kohler, and P. H a nggi, Phys. Rev. Lett. **90**, 210602 (2003).
[26] D.S. Fisher and P.A. Lee, Phys. Rev. B **23**, 6851 (1981).